Comparison of PD, PID and Sliding-Mode Position Controllers for V–Tail Quadcopter Stability

**JOSÉ J. CASTILLO-ZAMORA[1], KARLA A. CAMARILLO-GÓMEZ[2],
GERARDO I. PÉREZ-SOTO[3], (Member, IEEE), AND
JUVENAL RODRÍGUEZ-RESÉNDIZ[3], (Senior Member, IEEE)**

[1]Mechatronics Engineering Department, Tecnológico Nacional de México en Celaya, Celaya 38010, Mexico
[2]Mechanical Engineering Department, Tecnológico Nacional de México en Celaya, Celaya 38010, Mexico
[3]Faculty of Engineering, Universidad Autónoma de Querétaro, Santiago de Querétaro 76010, Mexico

Corresponding author: Juvenal Rodríguez-Reséndiz (juvenal@ieee.org)

ABSTRACT In this paper, a comparison of PD, PID, and SMC position controllers for a V-tail quadcopter is presented. First, a customized design of the V-tail quadcopter is shown to know the parameters of this structure and compare them with the commonly $\times$ structure quadcopter used in most papers. Then, the dynamic analysis of the V-tail quadcopter using the Newton–Euler formulation is presented. The main contribution of this paper remains in the design and Lyapunov stability analysis of the PD, PID, and SMC position controllers for the V-tail quadcopter because the robot manipulator methodology was used, treating the V-tail quadcopter as a robot manipulator. The simulation results validate the proposed controllers and algorithms for the V-tail quadcopter when the three controllers reach the desired position. Also, a non-conventional variable is introduced to study the stability analysis of unmanned aerial vehicles when controlled by PID position controller. Finally, a comparison between the three designed controllers for the V-tail quadcopter is presented, where the differences between each can be appreciated. So that, for the first time, three controllers for the V-tail quadcopter designed using the robot manipulator theory is presented.

INDEX TERMS V-tail quadcopter, PID controller, PD controller, sliding-mode controller, Lyapunov stability analysis.

I. INTRODUCTION

In the last decade, interest in unmanned aerial vehicles (UAVs) and their design and control has exponentially increased, due to their capability to carry out several complex tasks, in addition to their low–cost production and relatively simple operation [1].

Quadcopters have captured the attention of researchers because of their reduced dimensions, light–weight, mechanical structure, autonomy and their outstanding ability to efficiently complete assigned tasks. This kind of UAVs is classified as vertical take–off and landing, VTOL, due to their operation method [1], [2].

Several areas of science, as well as specific techniques and theories, are being adapted explicitly to quadcopters, resulting in a widely expanding research activity. To mention some areas of research involved in the manufacture and the development of aerial vehicles, we could cite aerodynamics, materials science, control theory, computer science, mechanical design, fluid dynamics, and microprocessors [1].

An observation can infer, quadcopter has a simple mechanical structure, but the control theory is not simple, due to the non–linear dynamics of the vehicle. It has 6 degrees of freedom (DOF) and only four actuators, which makes it a complex system to study and control [3].

It is important to obtain its dynamic model to study the vehicle. For this, two formulations are used: the Newton–Euler formulation [2]–[11], [21] and the Euler–Lagrange formulation [12]. The former is most commonly used to obtain the dynamic model of quadcopters, due to the simplicity of its equations, but this is not the case for a robot manipulators, where the Euler–Lagrange formulation is more convenient to implement.

The basic tasks of these UAVs are to reach stability and to follow the desired trajectory even if it is a single quadrotor task [11] or a multiple quadrotor task [21], so that is why there are many documented studies about these two main topics. Regarding the first one, algorithms to stabilize the orientation of a quadcopter keeping a predefined distance

from the ground have been developed by Khatoon *et al.* [7], Jeong and Jung [9], Jithu and Jayasree [12], Yang *et al.* [13], Walid *et al.* [14], Fernando *et al.* [15], and Lee *et al.* [16], also, altitude stabilization has been explained in [2], [3], [8], and [17]. In most of the studies taken as references for this paper, algorithms to stabilize the orientation of the vehicle are presented due to their direct formulation, and they give a dynamic model for the UAV. To execute this task, several and different methodologies have been adopted including sliding–mode control (SMC) [17] and even the well–known PD (proportional–derivative) [12], [14] and PID (proportional–integral–derivative) [2]–[4], [7], [8], [13] controllers. The latter is the most commonly used for stability analysis. All these techniques have been applied to typical cross–structure quadcopters (× structure) but not for V–tail quadcopters [6] as shown in this paper. Many techniques have been used to design PID controllers [2]–[4], [7], [8], [13], and each of them has their advantages and disadvantages.

In this paper, the dynamic analysis using Newton-Euler formulation for customized design of a V–tail quadcopter is presented to know the parameters of this structure and compare them with the × structure quadcopter used in most papers. The main contribution of this paper remains in the design and Lyapunov stability analysis of the PD, PID and SMC position controllers for the V–tail quadcopter because the robot manipulator methodology was used for that purposes [18]. The simulation results validate the proposed controllers and algorithms for the V–tail quadcopter when the three controllers reach the desired position. Also, a non-conventional variable is introduced to study the stability analysis of unmanned aerial vehicles when controlled by PID position controller. Finally, a comparison between the three designed controllers for a V–tail quadcopter is presented, where the differences between each can be appreciated. It is important to mention that in previous studies reviewed by the authors and given in the References section, this particular theory has never been implemented for UAV control.

II. COORDINATE REFERENCE FRAMES AND GEOMETRIC DESCRIPTION OF THE V–TAIL QUADCOPTER

In this section, a description of a V–tail quadcopter is given. Also, a description of each geometric parameter as well as the coordinate reference frames, which are important for understanding the dynamics of the vehicle, are given.

In mobile robotics, two different coordinate reference frames are needed to control the robot. The first reference frame is the so–called earth–fixed reference frame (O_{XYZ}), which is considered to be inertial and its origin stays fixed to a specific point in space. The second one is a mobile reference frame ($O_{X'Y'Z'}$), and its origin is fixed to the center of mass of the vehicle (Fig. 1), which implies that this reference frame moves with the quadcopter. It is used to determine the position and orientation of the V–tail in space [4]. The position of the quadcopter is described in the earth–fixed reference frame by the vector $\boldsymbol{\xi} = [x \, y \, z]^T \in \mathbb{R}^3$.

The orientation is fully described by the Euler angles contained in the vector $\boldsymbol{\eta} = [\phi \, \theta \, \psi]^T \in \mathbb{R}^3$, also known as *roll*, *pitch* and *yaw* angles, respectively [4], [5].

Figure 1 shows a V–tail quadcopter. It is named because its rear links can be adapted so that they form a ''V'' [6], with β being the angle of orientation of the links. All the geometric parameters considered in the further analysis are shown in Fig. 2 and 3, which represent the rear view and the top view, respectively. Descriptions of these parameters are introduced in Table 1.
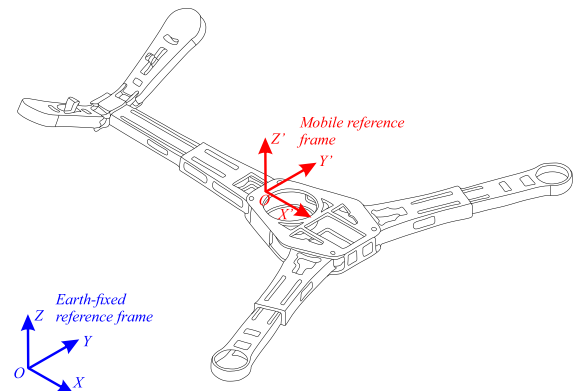

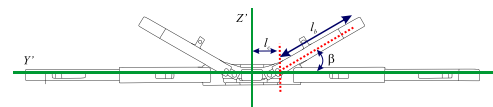**Figure 1.** Coordinate reference frames.

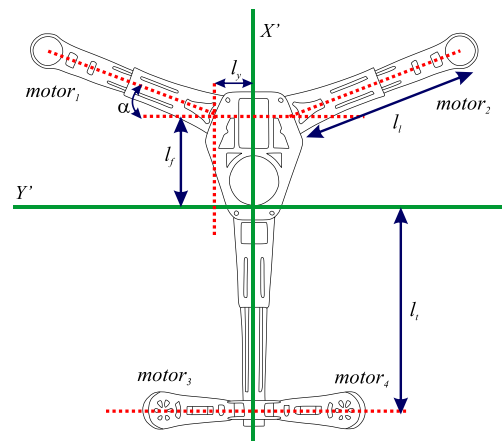**Figure 2.** Rear view of the V–tail quadcopter.

Figure 3. Top view of the V–tail quadcopter.

III. NEWTON–EULER FORMULATION FOR A RIGID BODY WITH 6 DOFS

In this section, the Newton–Euler formulation to obtain the dynamic model of a rigid body with 6 DOFs is introduced. The adaptation of this formulation to the quadcopter will be shown in upcoming sections.

TABLE 1. Description of the geometric parameters of the V–tail quadcopter.

Parameter	Description
α	Orientation angle of the front links
β	Orientation angle of the back links
l_b	Length of the back link
l_c	Distance in Y' from the origin of $O_{X'Y'Z'}$ to the beginning of the back link
l_f	Distance in X' from the origin of $O_{X'Y'Z'}$ to the beginning of the front link
l_l	Length of the front link
l_t	Distance in X' from the origin of $O_{X'Y'Z'}$ to motors 3 and 4
l_y	Distance in Y' from the origin of $O_{X'Y'Z'}$ to the beginning of the front link

The Newton–Euler formulation offers equations that describe the translational and rotational dynamics of a rigid body. These equations are derived from the first Euler axiom for Newton's second law and are represented by Tanveer *et al.* [2], Li and Li [3], Ahmed *et al.* [4], Khatoon *et al.* [7], Ahmed *et al.* [8], and Jeong and Jung [9]:

$$\begin{bmatrix} \widetilde{M} & 0 \\ 0 & \widetilde{I} \end{bmatrix} \begin{bmatrix} \dot{v} \\ \dot{\omega} \end{bmatrix} + \begin{bmatrix} \omega \times \widetilde{M} \cdot v \\ \omega \times \widetilde{I} \cdot \omega \end{bmatrix} = \begin{bmatrix} \kappa \\ \tau \end{bmatrix} \tag{1}$$

where $\widetilde{M}, \widetilde{I} \in \mathbb{R}^{3\times3}$ represent the mass and inertia tensors, respectively (notice that $\widetilde{\cdot}$ is only used to represent a tensor, establishing the difference between a matrix and a tensor), $0 \in \mathbb{R}^{3\times3}$ is the zero matrix. The vectors $\kappa \in \mathbb{R}^3$ and $\tau \in \mathbb{R}^3$ describe the forces and moments acting on the body, respectively, and are given in the mobile reference frame. The vector $v = [u\ v\ w]^T \in \mathbb{R}^3$ represents the linear velocity of the body expressed in the mobile reference frame, which is related to the velocity of the earth–fixed reference frame $\dot{\xi}$ (time derivative of vector ξ, see [2], [3], [7]–[11]) such that

$$\dot{\xi} = Rv.$$

where $R \in \mathbb{R}^{3\times3}$ is the rotational matrix corresponding to an absolute representation in relation to the earth–fixed reference frame, given in [2], [3], and [7]–[11] as:

$$R = \begin{bmatrix} C_\theta C_\psi & S_\phi S_\theta C_\psi - C_\phi S_\psi & C_\phi S_\theta C_\psi + S_\phi S_\psi \\ C_\theta S_\psi & S_\phi S_\theta S_\psi + C_\phi C_\psi & C_\phi S_\theta S_\psi - S_\phi C_\psi \\ -S_\theta & C_\theta S_\phi & C_\theta C_\phi \end{bmatrix}$$

where, from here to the end of the paper $C_a = \cos(a)$, $S_a = \sin(a)$.

In the same way, the angular velocity of the mobile reference frame is expressed by the vector $\omega = [p\ q\ r]^T \in \mathbb{R}^3$, which can be related to the roll, pitch and yaw velocities and, it depends on $\dot{\eta}$ (the time derivative of vector η), as shown in [2], [3], [7]–[10], and [12], by the following relation:

$$\omega = T\dot{\eta}$$

where T is a transformation matrix, presented in [2], [3], [7]–[10], and [12] and shown next:

$$T = \begin{bmatrix} 1 & 0 & -S_\theta \\ 0 & C_\phi & S_\phi C_\theta \\ 0 & -S_\phi & C_\phi C_\theta \end{bmatrix} \in \mathbb{R}^{3\times3} \tag{2}$$

Equation (1) corresponds to a dynamic model of a rigid body with 6 DOFs that depend on the linear and angular velocities and accelerations of the body expressed in the mobile reference frame. For convenience, an equation involving linear velocities and accelerations of the body with respect to the earth-fixed reference frame, and the angular velocities and accelerations of the body expressed in the mobile reference frame is presented to simplify the analysis [2], [3], [7]–[9], [11], [12]. The benefit of making this rearrangement of equation (1) is that the inertia tensor $\widetilde{I}$ is not dependent on time [7]. Moreover, the equation of linear movement is simplified in comparison with the equations obtained when considering the linear velocities and accelerations in the mobile reference frame. So, after modifying equation (1), the following result is obtained:

$$\begin{bmatrix} \widetilde{M} & 0 \\ 0 & \widetilde{I} \end{bmatrix} \begin{bmatrix} \ddot{\xi} \\ \dot{\omega} \end{bmatrix} + \begin{bmatrix} 0 \\ \omega \times \widetilde{I} \cdot \omega \end{bmatrix} = \begin{bmatrix} f \\ \tau \end{bmatrix} \tag{3}$$

Equation (3) combines the dynamics of the body in the earth–fixed reference frame and in the mobile reference frame. Herein, the vector $f \in \mathbb{R}^3$ appears, representing the external forces acting on the body described in the earth–fixed reference frame, the vector $0 \in \mathbb{R}^3$ represents the zero vector, and $\ddot{\xi}$ is the vector of linear accelerations in the earth–fixed reference frame.

IV. DYNAMIC MODEL OF THE V–TAIL QUADCOPTER
Until this point, the Newton–Euler formulation used to obtain the dynamic model of a rigid body has been described. Now it is important to adapt it to the V–tail quadcopter, considering the effects of the phenomena that affect the movement of the vehicle.

Taking as reference equation (3) and taking into account the effect of gravity on the vehicle, the dynamic model of the vehicle can be expressed, as shown in [18], as:

$$\widetilde{M}_t \begin{bmatrix} \ddot{\xi} \\ \dot{\omega} \end{bmatrix} + C(\dot{\xi}, \omega) \begin{bmatrix} \dot{\xi} \\ \omega \end{bmatrix} + \begin{bmatrix} G \\ 0 \end{bmatrix} = \begin{bmatrix} f \\ \tau \end{bmatrix} \tag{4}$$

where

$$\widetilde{M}_t = \begin{bmatrix} \widetilde{M} & 0 \\ 0 & \widetilde{I} \end{bmatrix} = \begin{bmatrix} m & 0 & 0 & 0 & 0 & 0 \\ 0 & m & 0 & 0 & 0 & 0 \\ 0 & 0 & m & 0 & 0 & 0 \\ 0 & 0 & 0 & I_{xx} & I_{xy} & I_{xz} \\ 0 & 0 & 0 & I_{yx} & I_{yy} & I_{yz} \\ 0 & 0 & 0 & I_{zx} & I_{zy} & I_{zz} \end{bmatrix}$$

$$C(\dot{\xi}, \omega) = \begin{bmatrix} 0 & 0 & 0 & 0 & 0 & 0 \\ 0 & 0 & 0 & 0 & 0 & 0 \\ 0 & 0 & 0 & 0 & 0 & 0 \\ 0 & 0 & 0 & 0 & A & -B \\ 0 & 0 & 0 & -A & 0 & C \\ 0 & 0 & 0 & B & -C & 0 \end{bmatrix}$$

$$G = \begin{bmatrix} 0 \\ 0 \\ mg \end{bmatrix} \tag{5}$$

where $\widetilde{M}_t \in \mathbb{R}^{6\times6}$ is the total mass tensor of the system, which includes the mass tensor $\widetilde{M}$ and the inertia tensor $\widetilde{I}$, $C(\dot{\xi},\omega) \in \mathbb{R}^{6\times6}$ is the Coriolis and centripetal effects matrix [2], [3], [7]–[9], [12], [18], m is the quadcopter mass, I_{ii} are the moments of inertia and g is the gravitational constant in the International System, and, according to [7] and [12], A, B, and C are such that:

$$A = I_{zx}p + I_{zy}q + I_{zz}r$$
$$B = I_{yx}p + I_{yy}q + I_{yz}r$$
$$C = I_{xx}p + I_{xy}q + I_{xz}r$$

The vector of external forces f includes the vector of lifting forces produced by each motor $f_m \in \mathbb{R}^3$, which is described in the mobile reference frame, and the vector of drag forces $f_D \in \mathbb{R}^3$ that acts in the opposite direction of the movement and is described in the earth–fixed reference frame. So, f can be defined as [4], [11]–[13], [17]

$$f = Rf_m - f_D$$

Considering that each motor produces a lifting force f_{m_i}, and taking into account the geometry of the model, the vector f_m can be defined by the addition of forces:

$$f_m = \begin{bmatrix} 0 \\ (f_{m_4} - f_{m_3})S_\beta \\ f_{m_1} + f_{m_2} + (f_{m_3} + f_{m_4})C_\beta \end{bmatrix} \quad (6)$$

where the magnitudes of the forces f_{m_i} are computed from the lift theory for the helicopter's propellers (see [4], [11]–[13], [17], [19]). So, the equation describing this quantity is given by:

$$f_{m_i} = \frac{\rho A_s C_T R^2 \omega_i^2}{2} = b\omega_i^2$$

where ρ is the air density, A_s the effective blades area, C_T the lift coefficient, R is blades radius and ω_i is the angular velocity of the blades of motor i.

The drag forces are expressed in the earth–fixed reference frame because they depend directly and only on the linear velocities of the vehicle given in the mentioned reference frame [13], [17], [19]:

$$f_D = \frac{\rho}{2}\|\dot{\xi}\|^T A C_D \dot{\xi} = \begin{bmatrix} f_{D_x} \\ f_{D_y} \\ f_{D_z} \end{bmatrix}$$

where $A \in \mathbb{R}^{3\times3}$ is the diagonal matrix of contact areas and $C_D \in \mathbb{R}^{3\times3}$ is the diagonal matrix of drag coefficients, which can be computed as shown in [19].

Three main effects compose the vector of moments acting on the vehicle, τ, with respect to the mobile reference frame: moments produced by lifting forces (generated by motors), τ_{f_m}; torques produced by the motors, τ_m; and gyroscopic effects, τ_g, which can be written as [4], [7], [11]–[13]:

$$\tau = \tau_{f_m} + \tau_m + \tau_g$$

The vector τ_{f_m} contains the moments produced by the lifting force related to the center of mass of the vehicle and can be expressed as:

$$\tau_{f_m} = \begin{bmatrix} (f_{m_1} - f_{m_2})(l_y + l_l C_\alpha) + (f_{m_3} - f_{m_4})(l_c C_\beta + l_b) \\ -(f_{m_1} + f_{m_2})(l_f + l_l S_\alpha) + (f_{m_3} + f_{m_4})(l_t C_\beta) \\ (f_{m_3} - f_{m_4})(l_t S_\beta) \end{bmatrix} \quad (7)$$

It is known that the motors produce a free moment due to the rotation around their own axes [4], [7], [11]–[13], which is a function of the angular velocity. This phenomenon is represented in the vector τ_m as follows:

$$\tau_m = \begin{bmatrix} 0 \\ (\tau_{m_3} - \tau_{m_4})S_\beta \\ \tau_{m_1} - \tau_{m_2} + (-\tau_{m_3} + \tau_{m_4})C_\beta \end{bmatrix} \quad (8)$$

The magnitude of the i–th moment τ_{m_i} according to [4], [7], [11]–[13], and [19], is given by:

$$\tau_{m_i} = \frac{\rho A_t C_Q R^3 \omega_i^2}{2} = d\omega_i^2$$

where A_t is the transverse section area of the blade and C_Q is the torque coefficient. The sign of the moment is selected according to the sense of rotation of the blades.

The vector of moments caused by the gyroscopic effects can be expressed as [4], [11], [12], [17]:

$$\tau_g = -\sum_{i=1}^{4} J_{tp} \left(\omega \times \begin{bmatrix} 0 \\ 0 \\ 1 \end{bmatrix} \right) \omega_i$$

where J_{tp} is the rotational moment of inertia of the motor around its own axis.

Notice that all of these vectors are expressed in the mobile reference frame, so the vector τ is expressed in the same reference frame.

Due to the non–linearity of the system and the number of unknown parameters and terms, it is necessary to simplify the dynamic model when designing the controllers.

A. SIMPLIFIED DYNAMIC MODEL OF THE V–TAIL QUADCOPTER

As mentioned in the previous paragraph, it is necessary to make some simplifications to the dynamic model presented in equation (4) when designing the controllers. These simplifications are examined in this section.

First, the product of the Coriolis and centripetal effects matrix $C(\dot{\xi},\omega)$ and the velocity vector $[\dot{\xi}\ \omega]^T$ is neglected due to the magnitude of the resultant vector is smaller than the other terms of the dynamic model. The same is true for the gyroscopic effects, which are also neglected. Assuming that the V–tail quadcopter operates in a quasi–stationary region, i.e., $\phi \approx 0$ and $\theta \approx 0$, it can be established that $\dot{\eta} = \omega$ and $\ddot{\eta} = \dot{\omega}$, which can be easily proved if $\phi = 0$ and $\theta = 0$ are substituted into the transformation matrix T, introduced in equation (2). The third and last simplification consists of assuming that the quadcopter operates at low speeds, so that,

drag effects can be neglected, i.e., $f_D = 0$. Also, for this reason, coupling effects are not taken into consideration. All these assumptions have been proven in [3], [4], [7], [9]–[11], [14], [15], [20], where further information about these facts is given. Finally, and considering the dynamic model of equation (4), the modified dynamic model of the vehicle is

$$\widetilde{M}_t \begin{bmatrix} \ddot{\xi} \\ \ddot{\eta} \end{bmatrix} + \begin{bmatrix} G \\ 0 \end{bmatrix} = \begin{bmatrix} R f_m \\ \tau_{f_m} + \tau_m \end{bmatrix}$$

To simplify the vector f_m, given in (6), and the vectors of external moments τ_{f_m} and τ_m, introduced in (7) and (8), respectively, the angle β is set to 0, so the modified vectors are

$$f = \begin{bmatrix} 0 \\ 0 \\ f_{m_1} + f_{m_2} + f_{m_3} + f_{m_4} \end{bmatrix} \quad (9)$$

$$\tau = \begin{bmatrix} (f_{m_1} - f_{m_2})(l_y + l_l C_\alpha) + (f_{m_3} - f_{m_4})(l_c + l_b) \\ -(f_{m_1} + f_{m_2})(l_f + l_l S_\alpha) + (f_{m_3} + f_{m_4})(l_t) \\ \tau_{m_1} - \tau_{m_2} - \tau_{m_3} + \tau_{m_4} \end{bmatrix} \quad (10)$$

Besides the simplification of the vectors, β is set to 0 to get an approximation of the V–tail quadcopter behavior because there was no information about it.

Considering equations (9) and (10), the control variables of the quadcopter are defined as follows [3], [15]:

$$U_1 = f_{m_1} + f_{m_2} + f_{m_3} + f_{m_4} \quad (11)$$
$$U_2 = (f_{m_1} - f_{m_2})(l_y + l_l C_\alpha) + (f_{m_3} - f_{m_4})(l_c + l_b) \quad (12)$$
$$U_3 = -(f_{m_1} + f_{m_2})(l_f + l_l S_\alpha) + (f_{m_3} + f_{m_4})(l_t) \quad (13)$$
$$U_4 = \tau_{m_1} - \tau_{m_2} - \tau_{m_3} + \tau_{m_4} \quad (14)$$

The inertia tensor $\widetilde{I}$ in (5), is simplified if it is considered that the main axis of inertia coincides with the axis of the mobile reference frame (see the design and configuration of the V–tail described in Section II). This simplification is proved by the data obtained from the CAD software used to create the prototype of the quadcopter. Here it can be found that the main inertia moments are of the order of 10^{-3} kg · m^2. The other components of the inertia tensor are of the order of 10^{-7} kg · m^2, which can be mathematically expressed as:

$$\widetilde{I} = \begin{bmatrix} I_{xx} & 0 & 0 \\ 0 & I_{yy} & 0 \\ 0 & 0 & I_{zz} \end{bmatrix}$$

Modifying, in this sense, the total mass tensor, $\widetilde{M}_t$, of equation (5), the final modified dynamic model is given by [21]:

$$\begin{bmatrix} m\ddot{x} \\ m\ddot{y} \\ m\ddot{z} \\ I_{xx}\ddot{\phi} \\ I_{yy}\ddot{\theta} \\ I_{zz}\ddot{\psi} \end{bmatrix} + \begin{bmatrix} 0 \\ 0 \\ mg \\ 0 \\ 0 \\ 0 \end{bmatrix} = \begin{bmatrix} U_x U_1 \\ U_y U_1 \\ U_z U_1 \\ U_2 \\ U_3 \\ U_4 \end{bmatrix} \quad (15)$$

where $U_x = C_\phi S_\theta C_\psi + S_\phi S_\psi$, $U_y = C_\phi S_\theta S_\psi - S_\phi C_\psi$ and $U_z = C_\phi C_\theta$, and which are used to design the controller and carry out the corresponding simulations.

V. DESIGN OF THE PID POSITION CONTROLLER BASED ON THE CONTROL THEORY OF ROBOT MANIPULATORS

In this section, the procedure to design the PID controller is described. The procedure presented is based on the method established in [18].

Now it is essential to define the vector $q \in \mathbb{R}^6$ as:

$$q = \begin{bmatrix} \xi \\ \eta \end{bmatrix}$$

Then the system state is defined by the vector $\Xi \in \mathbb{R}^{18}$ described as:

$$\Xi = \begin{bmatrix} \zeta \in \mathbb{R}^6 \\ \tilde{q} \\ \dot{q} \end{bmatrix} \quad (16)$$

such that $\dot{\zeta} = \tilde{q}$, $\tilde{q}_i = q_{d_i} - q_i$ and $\dot{\tilde{q}} = -\dot{q}$ where q_{d_i} is the set point (in this case, strictly constant).

The PID control law is given by:

$$\begin{bmatrix} f \\ \tau \end{bmatrix} = K_p \tilde{q} + K_v \dot{\tilde{q}} + K_i \zeta$$

where $K_p, K_v, K_i \in \mathbb{R}^{6\times6}$ are the diagonal matrices of proportional, derivative and integral gains, respectively.

Thus, the closed–loop equation of the system (16) is obtained:

$$\ddot{q} = \begin{bmatrix} \left(K_{p_x}\tilde{x} - K_{v_x}\dot{x} + K_{i_x}\zeta_x\right)/m \\ \left(K_{p_y}\tilde{y} - K_{v_y}\dot{y} + K_{i_y}\zeta_y\right)/m \\ \left(K_{p_z}\tilde{z} - K_{v_z}\dot{z} + K_{i_z}\zeta_z - mg\right)/m \\ \left(K_{p_\phi}\tilde{\phi} - K_{v_\phi}\dot{\phi} + K_{i_\phi}\zeta_\phi\right)/I_{xx} \\ \left(K_{p_\theta}\tilde{\theta} - K_{v_\theta}\dot{\theta} + K_{i_\theta}\zeta_\theta\right)/I_{yy} \\ \left(K_{p_\psi}\tilde{\psi} - K_{v_\psi}\dot{\psi} + K_{i_\psi}\zeta_\psi\right)/I_{zz} \end{bmatrix}, \quad (17)$$

which corresponds to the control law to be implemented on the quadcopter based on the dynamic model of equation (15).

A. STABILITY ANALYSIS USING A LYAPUNOV FUNCTION
Following the procedure in [18], it is necessary to make a change of variables, i.e.:

$$\mu = \begin{bmatrix} \mu_x \\ \mu_y \\ \mu_z \\ \mu_\phi \\ \mu_\theta \\ \mu_\psi \end{bmatrix} = \begin{bmatrix} \zeta_x \\ \zeta_y \\ \zeta_z - K_{i_z}^{-1} mg \\ \zeta_\phi \\ \zeta_\theta \\ \zeta_\psi \end{bmatrix}$$

Then, the new vector of states $\Xi_n \in \mathbb{R}^{18}$ is given by:

$$\Xi_n = \begin{bmatrix} \mu \\ \tilde{q} \\ \dot{q} \end{bmatrix}$$

where

$$\frac{d}{dt}\begin{bmatrix} \mu \\ \tilde{q} \\ \dot{q} \end{bmatrix} = \begin{bmatrix} \tilde{q} \\ -\dot{q} \\ \ddot{q} \end{bmatrix} \quad (18)$$

so that, the vector $\ddot{q}$ is:

$$\ddot{q} = \begin{bmatrix} \left(K_{p_x}\tilde{x} - K_{v_x}\dot{x} + K_{i_x}\mu_x\right)/m \\ \left(K_{p_y}\tilde{y} - K_{v_y}\dot{y} + K_{i_y}\mu_y\right)/m \\ \left(K_{p_z}\tilde{z} - K_{v_z}\dot{z} + K_{i_z}\mu_z\right)/m \\ \left(K_{p_\phi}\tilde{\phi} - K_{v_\phi}\dot{\phi} + K_{i_\phi}\mu_\phi\right)/I_{xx} \\ \left(K_{p_\theta}\tilde{\theta} - K_{v_\theta}\dot{\theta} + K_{i_\theta}\mu_\theta\right)/I_{yy} \\ \left(K_{p_\psi}\tilde{\psi} - K_{v_\psi}\dot{\psi} + K_{i_\psi}\mu_\psi\right)/I_{zz} \end{bmatrix}$$

This guarantees that the only equilibrium point of the system is the origin. Whit regard to the stability analysis of the PID controller, the next global change of variables is established:

$$\begin{bmatrix} \gamma \\ \tilde{q} \\ \dot{q} \end{bmatrix} = \begin{bmatrix} \epsilon I & I & 0 \\ 0 & I & 0 \\ 0 & 0 & I \end{bmatrix} \begin{bmatrix} \mu \\ \tilde{q} \\ \dot{q} \end{bmatrix} = \begin{bmatrix} \epsilon\mu + \tilde{q} \\ \tilde{q} \\ \dot{q} \end{bmatrix} \quad (19)$$

with $\epsilon > 0$ being a new parameter, introduced to analyze the stability of the UAV. $I \in \mathbb{R}^{6\times 6}$ is the identity matrix. Note that this parameter ϵ is a characteristic used in control theory of robot manipulators, which is applied in this paper. The new variable vector γ is also introduced in equation (19), as suggested in [18], this variable has never been used before in the stability analysis of quadcopters because it belongs to the control theory of robot manipulators.

So the closed–loop equation is then obtained as:

$$\frac{d}{dt}\begin{bmatrix} \gamma \\ \tilde{q} \\ \dot{q} \end{bmatrix} = \begin{bmatrix} \epsilon\tilde{q} - \dot{q} \\ -\dot{q} \\ \ddot{q} \end{bmatrix}$$

where

$$\ddot{q} = \widetilde{M}_t^{-1}\left[K_p\tilde{q} - K_v\dot{q} + \frac{1}{\epsilon}K_i(\gamma - \tilde{q})\right]$$

$$= \widetilde{M}_t^{-1}\left[\left(K_p - \frac{1}{\epsilon}K_i\right)\tilde{q} - K_v\dot{q} + \frac{1}{\epsilon}K_i\gamma\right] \quad (20)$$

Equation (20) is autonomous, and its origin is the only equilibrium point; besides, due to the globality of the variable change (19), the attributes of stability of this equilibrium correspond to the ones of the equilibrium of equation (18).

The Lyapunov candidate function proposed for the stability analysis is:

$$V(\tilde{q}, \dot{q}, \gamma) = \frac{1}{2}\begin{bmatrix} \gamma \\ \tilde{q} \\ \dot{q} \end{bmatrix}^T \begin{bmatrix} \frac{1}{\epsilon}K_i & 0 & 0 \\ 0 & \epsilon K_v & -\epsilon\widetilde{M}_t \\ 0 & -\epsilon\widetilde{M}_t & \widetilde{M}_t \end{bmatrix} \begin{bmatrix} \gamma \\ \tilde{q} \\ \dot{q} \end{bmatrix}$$
$$+ \frac{1}{2}\tilde{q}^T\left[K_p - \frac{1}{\epsilon}K_i\right]\tilde{q} + U(q_d - \tilde{q})$$
$$- U(q_d) + \tilde{q}^T\begin{bmatrix} G \\ 0 \end{bmatrix} \quad (21)$$

where $U(q)$ represents the potential energy of the quadcopter.

The Lyapunov candidate function (21) is positive–definite if ϵ is chosen in a way that the following condition is true:

$$\frac{\lambda_{min}\{K_v\}\,\lambda_{min}\{\widetilde{M}_t\}}{\lambda_{max}^2\{\widetilde{M}_t\}} > \epsilon > \frac{\lambda_{max}\{K_i\}}{\lambda_{min}\{K_p\}}$$

and it can be proved that the time derivative of the Lyapunov candidate function of equation (21) satisfies the condition:

$$\dot{V}(\tilde{q}, \dot{q}, \gamma) \leq -\begin{bmatrix} \|\tilde{q}\| \\ \|\dot{q}\| \end{bmatrix}^T \begin{bmatrix} \Lambda_{11} & 0 \\ 0 & \Lambda_{22} \end{bmatrix} \begin{bmatrix} \|\tilde{q}\| \\ \|\dot{q}\| \end{bmatrix}$$

with

$$\Lambda_{11} = \epsilon\lambda_{min}\{K_p\} - \lambda_{max}\{K_i\}$$
$$\Lambda_{22} = \lambda_{min}\{K_v\} - \epsilon\lambda_{max}\{\widetilde{M}_t\}$$

So that the time derivative of the Lyapunov candidate function is negative–definite if ϵ is selected to satisfy the following condition:

$$\frac{\lambda_{min}\{K_v\}}{\lambda_{max}\{\widetilde{M}_t\}} > \epsilon > \frac{\lambda_{max}\{K_i\}}{\lambda_{min}\{K_p\}}$$

If all the conditions over ϵ are satisfied, it can be ensured that the origin of the closed–loop equation (19) is a stable equilibrium point of the system [16], [18]. The LaSalle theorem needs to be applied in orderto prove the asymptotic stability of the origin. So, the set Ω is defined as:

$$\Omega = \left\{ \Xi_n \in \mathbb{R}^{18} : \dot{V}(\Xi_n) = 0 \right\}$$
$$= \left\{ \gamma \in \mathbb{R}^6, \tilde{q} = 0 \in \mathbb{R}^6, \dot{q} = 0 \in \mathbb{R}^6 \right\}$$

It is easily and immediately appreciated that $\dot{V}(\tilde{q}, \dot{q}, \gamma) = 0$ if and only if $\tilde{q} = 0$ and $\dot{q} = 0$. For the solution $\Xi_n(t)$ to belong to Ω for all $t \geq 0$, it is sufficient and necessary that $\tilde{q} = 0$ and $\dot{q} = 0$ for all $t \geq 0$; hence, also $\ddot{q} = 0$ must be satisfied for all $t \geq 0$. Then, it can be concluded that if $\Xi_n(t) \in \Omega$ for all $t \geq 0$, then $\gamma = 0$ for all $t \geq 0$. Therefore, $[\gamma^T\ \tilde{q}^T\ \dot{q}^T] = 0^T \in \mathbb{R}^{18}$ is the only initial condition in Ω for which $\Xi_n \in \Omega$ for all $t \geq 0$. From these statements, it can be assumed that the origin of the closed–loop equation (19) is an asymptotic stable equilibrium point.

VI. DESIGN OF THE PD POSITION CONTROLLER BASED ON THE CONTROL THEORY OF ROBOT MANIPULATORS

In this section, the design procedure for the PD controller is described. It is important to mention that the procedure followed is based on the control theory of robot manipulators explained in [18], similar to what has been shown in the previous section.

Considering the vectors q and $\tilde{q}$ previously established, the state of the system can be defined as:

$$\Gamma = \begin{bmatrix} \tilde{q} \\ \dot{q} \end{bmatrix} \in \mathbb{R}^{12} \quad (22)$$

By knowing that the PD control law is given by:

$$\begin{bmatrix} f \\ \tau \end{bmatrix} = K_p\tilde{q} - K_v\dot{q}$$

with K_p and K_v as defined in the previous section.

It is possible to define the closed–loop system (22) as:

$$\ddot{q} = \begin{bmatrix} \left(K_{p_x}\tilde{x} - K_{v_x}\dot{x}\right)/m \\ \left(K_{p_y}\tilde{y} - K_{v_y}\dot{y}\right)/m \\ \left(K_{p_z}\tilde{z} - K_{v_z}\dot{z} - mg\right)/m \\ \left(K_{p_\phi}\tilde{\phi} - K_{v_\phi}\dot{\phi}\right)/I_{xx} \\ \left(K_{p_\theta}\tilde{\theta} - K_{v_\theta}\dot{\theta}\right)/I_{yy} \\ \left(K_{p_\psi}\tilde{\psi} - K_{v_\psi}\dot{\psi}\right)/I_{zz} \end{bmatrix} \quad (23)$$

This equation corresponds to the control to be implemented on the quadcopter based on the dynamic model of equation (15).

A. STABILITY ANALYSIS USING A LYAPUNOV FUNCTION

Using the time derivative of equation (22) and letting this be equal to $0 \in \mathbb{R}^{12}$, the equilibrium of the system can be found. Since this equilibrium point is not equal to the origin of the system, it is necessary to make a change of variables in the manner that:

$$\delta = \begin{bmatrix} \delta_x \\ \delta_y \\ \delta_z \\ \delta_\phi \\ \delta_\theta \\ \delta_\psi \end{bmatrix} = \begin{bmatrix} \tilde{x} \\ \tilde{y} \\ \tilde{z} - K_{p_z}^{-1}mg \\ \tilde{\phi} \\ \tilde{\theta} \\ \tilde{\psi} \end{bmatrix}$$

So now, it is convenient to define a new vector of states $\Gamma_n \in \mathbb{R}^{12}$, such as:

$$\Gamma_n = \begin{bmatrix} \delta \\ \dot{q} \end{bmatrix} \quad (24)$$

where the origin of the system is the only equilibrium point of the system.

Let the Lyapunov candidate function be

$$V\left(\delta, \dot{q}\right) = \frac{1}{2} \begin{bmatrix} \delta \\ \dot{q} \end{bmatrix}^T \begin{bmatrix} K_p & 0 \\ 0 & \tilde{M}_t \end{bmatrix} \begin{bmatrix} \delta \\ \dot{q} \end{bmatrix}, \quad (25)$$

which is positive–definite since K_p and $\tilde{M}_t$ are positive–definite matrices. It can be proved that the time derivative of equation (25) is negative-definite in the manner that:

$$\dot{V}\left(\delta, \dot{q}\right) = - \begin{bmatrix} \delta \\ \dot{q} \end{bmatrix}^T \begin{bmatrix} 0 & 0 \\ 0 & K_v \end{bmatrix} \begin{bmatrix} \delta \\ \dot{q} \end{bmatrix}$$

where K_v is a positive–definite matrix.

With these two properties of the function shown in equation (25), it can be ensured that the origin of the system (24) is a stable equilibrium point. It is necessary to apply the LaSalle theorem in the same way that it was used for the PID controller to prove asymptotic stability.

Let the set Π be:

$$\Pi = \left\{ \Gamma_n \in \mathbb{R}^{12} : \dot{V}\left(\Gamma_n\right) = 0 \right\}$$
$$= \left\{ \delta \in \mathbb{R}^6, \dot{q} = 0 \in \mathbb{R}^6 \right\}$$

It is immediately apparent that $\dot{V}\left(\delta, \dot{q}\right) = 0$ if and only if $\dot{q} = 0$. For the solution $\Gamma_n(t)$ to belong to Π for all

$t \geq 0$, it is sufficient and necessary that $\dot{q} = 0$ for all $t \geq 0$; hence, also $\ddot{q} = 0$ must be satisfied for all $t \geq 0$. Taking this in consideration, it can be concluded that if $\Gamma_n(t) \in \Pi$ for all $t \geq 0$, then $\delta = 0$ for all $t \geq 0$. Therefore, $[\delta^T \ \dot{q}^T] = 0^T \in \mathbb{R}^{12}$ is the only initial condition in Π for which $\Gamma_n \in \Omega$ for all $t \geq 0$. From these statements, it can be assumed that the origin of the closed–loop equation (24) is an asymptotic stable equilibrium point.

VII. DESIGN OF THE SLIDING–MODE POSITION CONTROLLER

Sliding–mode controllers have been successfully adapted to UAVs as mentioned in [17]. In this section, the design of a controller of SMC is shown, based on the methodology found [17], while the stability analysis is carried out using the control theory of robot manipulators [18].

Let the sliding surfaces be defined and given in the vector $S \in \mathbb{R}^6$ as:

$$S = \begin{bmatrix} S_x \\ S_y \\ S_z \\ S_\phi \\ S_\theta \\ S_\psi \end{bmatrix} = \begin{bmatrix} \dot{\tilde{x}} + \lambda_x \tilde{x} \\ \dot{\tilde{y}} + \lambda_y \tilde{y} \\ \dot{\tilde{z}} + \lambda_z \tilde{z} \\ \dot{\tilde{\phi}} + \lambda_\phi \tilde{\phi} \\ \dot{\tilde{\theta}} + \lambda_\theta \tilde{\theta} \\ \dot{\tilde{\psi}} + \lambda_\psi \tilde{\psi} \end{bmatrix}$$

with $\lambda_i > 0$.

By knowing that $\dot{\tilde{q}} = -\dot{q}$, the sliding surfaces can be expressed as:

$$S = \begin{bmatrix} -\dot{x} + \lambda_x \tilde{x} \\ -\dot{y} + \lambda_y \tilde{y} \\ -\dot{z} + \lambda_z \tilde{z} \\ -\dot{\phi} + \lambda_\phi \tilde{\phi} \\ -\dot{\theta} + \lambda_\theta \tilde{\theta} \\ -\dot{\psi} + \lambda_\psi \tilde{\psi} \end{bmatrix} = -\dot{q} + K_l \tilde{q} \quad (26)$$

with $K_l \in \mathbb{R}^{6 \times 6}$ being the diagonal matrix of gains λ_i.

It is necessary to define the attractive sliding surfaces, which depend on the vector $\dot{S} \in \mathbb{R}^6$ such that:

$$\dot{S} = -K_k \text{ sign}\left(S\right) \quad (27)$$

where $K_k \in \mathbb{R}^{6 \times 6}$ is a diagonal matrix that depends on the gains of the controller. Satisfying this, the sliding condition $S^T \dot{S} \leq 0$.

By considering equation (26), the time derivative of the sliding surfaces vector S can also be expressed as:

$$\dot{S} = -\ddot{q} - K_l \dot{q} \quad (28)$$

Substituting equation (27) into equation (28) and solving for $\ddot{q}$, the following result can be obtained:

$$\ddot{q} = K_k \text{ sign}\left(S\right) - K_l \dot{q} \quad (29)$$

or in an extended form:

$$\begin{bmatrix} \ddot{x} \\ \ddot{y} \\ \ddot{z} \\ \ddot{\phi} \\ \ddot{\theta} \\ \ddot{\psi} \end{bmatrix} = \begin{bmatrix} K_{k_x}\,\text{sign}\,(S_x) - \lambda_x \dot{x} \\ K_{k_y}\,\text{sign}\,(S_y) - \lambda_y \dot{y} \\ K_{k_z}\,\text{sign}\,(S_z) - \lambda_z \dot{z} \\ K_{k_\phi}\,\text{sign}\,(S_\phi) - \lambda_\phi \dot{\phi} \\ K_{k_\theta}\,\text{sign}\,(S_\theta) - \lambda_\theta \dot{\theta} \\ K_{k_\psi}\,\text{sign}\,(S_\psi) - \lambda_\psi \dot{\psi} \end{bmatrix}$$

A. STABILITY ANALYSIS USING A LYAPUNOV FUNCTION

To analyze the stability of the system, let the Lyapunov candidate function be given as:

$$V(S) = \frac{1}{2} S^T S \tag{30}$$

where S was established in equation (26) and is also used to describe the state of the system.

It can be proved that the Lyapunov candidate function (30) is a local positive–definite function while the time derivative of it is local negative–definite function and is given as:

$$\dot{V}(S) = S^T \dot{S}$$

So, it can be guaranteed that the origin of the system is a stable equilibrium point. Now, to apply the LaSalle theorem, let the set Φ be defined as:

$$\Phi = \left\{ S \in \mathbb{R}^6 : \dot{V}(S) = 0 \right\} = \{ S = 0 \}$$

Herein, the only element of the set is the zero vector $\mathbf{0}$, which ensures the asymptotic stability of the origin.

VIII. SIMULATIONS AND RESULTS

With the three controllers designed and analyzed, a set of simulations was carried out to validate them. In this section, the simulations and the results of these are described.

The non–holonomic constraints between the linear accelerations with respect to the earth–fixed reference frame, and the yaw, roll and pitch angles [17] that related the objective control with the control variables [10], are given by:

$$S_\phi = \frac{\ddot{x} S_\psi - \ddot{y} C_\psi}{\sqrt{\ddot{x}^2 + \ddot{y}^2 + (\ddot{z} + g)^2}} \tag{31}$$

$$T_\theta = \frac{\ddot{x} C_\psi + \ddot{y} S_\psi}{\ddot{z} + g} \tag{32}$$

The block diagram of the algorithm for the PID and PD controllers is shown in Fig. 4, where it is possible to observe that there is an external control loop, which corresponds to the position control, and an inner control loop that controls the orientation of the quadcopter. Also, the block of non–holonomic constraints, where equations (31) and (32) were programmed, is considered.

To simulate the sliding–mode controller, the algorithm introduced in [17] was programmed. The block diagram of the algorithm is shown in Fig. 5.

Taking into consideration equations (20) and (23), as well as the control algorithm introduced in Fig. 4 and the parameters of Table 2 (where the values of b and d were taken
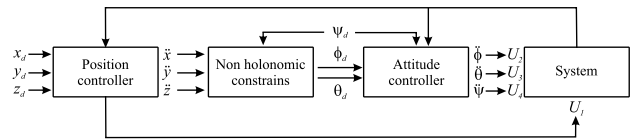

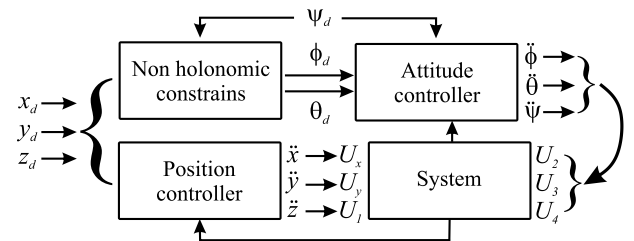**Figure 4.** Block diagram of the control algorithm for the PID and PD controllers.

Figure 5. Block diagram of the control algorithm for the SMC.

TABLE 2. Values of the parameters of the V–tail quadcopter for the simulations.

Parameter	Value	Parameter	Value
α	30°	b	4.95×10^{-5} N · s²
β	0°	d	7.5×10^{-7} N · m · s²
l_b	0.083 m	m	2.03 kg
l_c	0.04 m	g	9.81 m/s²
l_f	0.093 m	I_{xx}	2.547×10^{-3} kg · m²
l_l	0.185 m	I_{yy}	3.613×10^{-3} kg · m²
l_t	0.2 m	I_{zz}	1.074×10^{-3} kg · m²
l_y	0.04 m		

from [13]), the system was simulated in Matlab©. For the simulation of the SMC, the equation (29) and the algorithm introduced in Fig. 5 were taken into consideration. Moreover, for the simulation, $x_d = 1$ m, $y_d = -1$ m, $z_d = 2$ m and $\psi_d = 30°$.

Figure 6.a shows the time evolution of the position of the quadcopter in the X-axis, while Fig. 6.b and 6.c show how the quadcopter moves in the Y and Z directions, respectively.

From Fig. 6.a and 6.b, it can be established that the PD and PID controllers make the vehicle behave in the same manner (depending on the gains of these), but it does not occur the same with the sliding–mode controller. It can be seen that the PD and PID controllers have an exponential behavior while the sliding–mode controller has a linear behavior. Time stabilization is another remarkable characteristic of the controllers that can be modified by the gains of each but, from Fig. 6.a and 6.b, it could be inferred that the sliding–mode controller stabilizes the vehicle faster than the other two controllers do.

In Fig. 6.c, it can be observed that the sliding–mode controller makes the quadcopter reach the desired position faster than the PD and PID controllers. The similarity in behavior between the PD and PID controllers can be seen but also the difference regarding time stabilization. It is clear that the PD controller responds faster than the PID controller. Once again, it is important to mention that time stabilization,
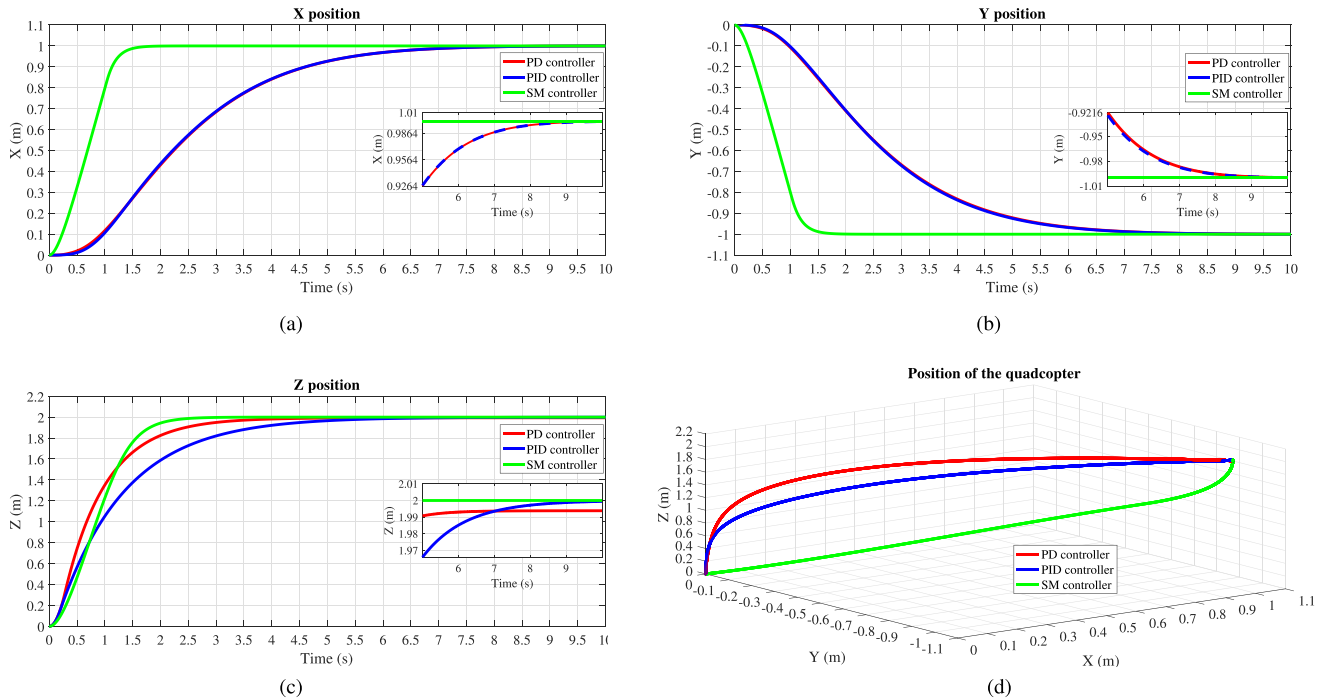
Figure 6. Position of the quadcopter for the three controllers: (a) *X*−position, (b) *Y*−position, (c) *Z*−position, (d) position in space.

as well as other properties of the closed–loop system can be modified by the gains of the controllers.

In Fig. 6.a, 6.b and 6.c, it is possible to appreciate the differences in the movements of the quadcopter between each of the controllers. In Fig. 6.d a comparison of the movement of the quadcopter in space is represented so that it is easier to get an idea of the possible real movement of it.

In Fig. 6.d, the differences in the movement of the quad-copter in the space with each controller with respect to the others can be appreciated. The linear behavior of the quadcopter with the sliding–mode controller is clearly dis-tinguished from the exponential behavior of the PD and PID controllers.

By observing the graphs a–c in Fig. 6, it can be seen that the three controllers tend to eliminate the error, but this does not happen with the movement in the *Z* direction, as shown in Fig. 6.c, where it can be seen that the SM and PID con-trollers can eliminate the error in the stable state but that the PD controller cannot. It is worth mentioning that this can affect the performance of the quadcopter when it comes to precision maneuvers, but this cannot be a problem depending on the application of the quadcopter.

For the yaw movement (ψ angle), Fig. 7 is obtained, where it can be appreciated how the quadcopter reaches the desired orientation. The SM controller takes the quadcopter to the specified angle in less time than the PD, and the PID controllers do. In the zoom of Fig. 7, it can be observed how the three controllers tend to eliminate the error when time increases.

The roll and pitch angles cannot be ignored since they affect the movement in the *Y* and *X* directions, respectively,
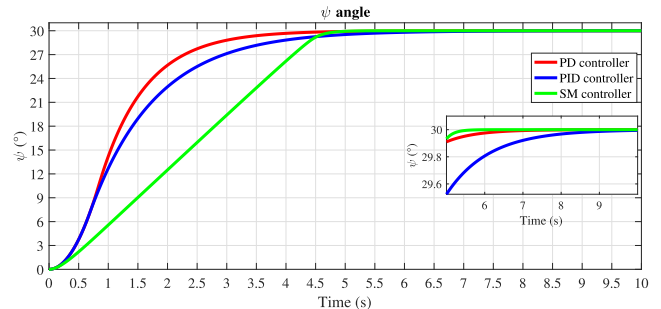

Figure 7. Yaw (ψ) angle of the quadcopter for the three controllers.
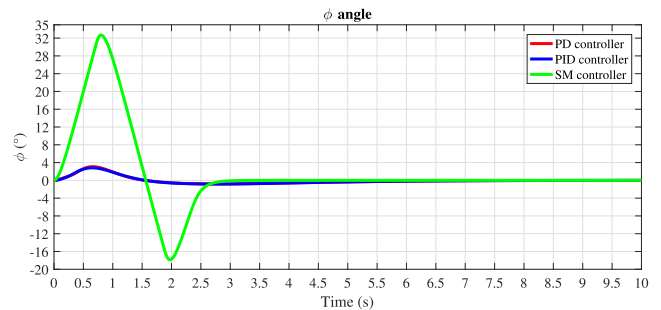

Figure 8. Roll (ϕ) angle of the quadcopter for the three controllers.

as can be appreciated from equations (31) and (32), so the behavior of these two variables is shown in Fig. 8 and 9.

In Fig. 8 and 9, it is easy to observe how the magnitude of the angles varies from one controller to another. For the SMC, the roll and pitch angles exceed 20°, making it possible to reach the desired position in less time than with the other
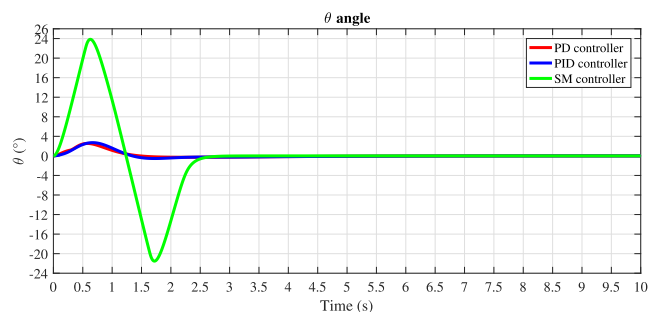
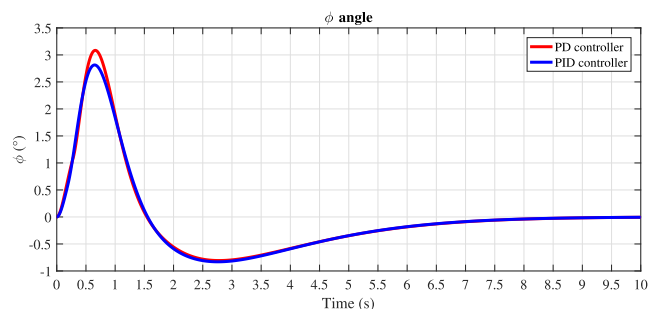**Figure 9.** Pitch (θ) angle of the quadcopter for the three controllers.

Figure 10. Roll (ϕ) angle resulted from the PD and PID controllers.
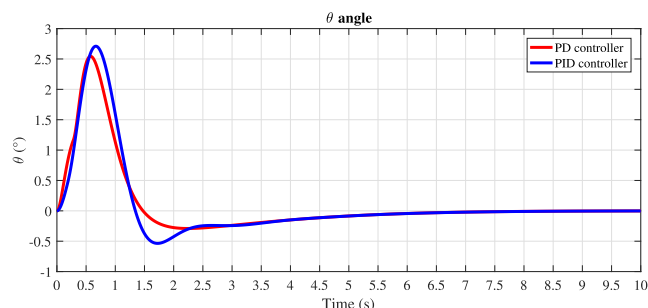

Figure 11. Pitch (θ) angle resulted from the PD and PID controllers.

two controllers. The higher the angles ϕ and θ, the faster the quadcopter moves in the Y and X directions, respectively; so that, since the quadcopter would not work in a stationary state, which makes the adopted simplifications to be wrong.

For the PD and PID controllers, it can be seen that the magnitude of the angles is so much smaller than for the SMC. Fig. 10 and 11 show the roll and pitch angles resulted from the PD and PID controllers for a better appreciation.

In both cases, the roll and pitch angles are near 3°, so it can be concluded that the quadcopter operates near the stationary state so that the simplifications previously made are valid. It can be observed that the angle ϕ has similar behavior for the two controllers, but the θ angle presents a slightly different behavior.

IX. CONCLUSIONS

In this paper, a dynamic model of a V–tail quadcopter was introduced, and an algorithm to control the position of this kind of vehicle with the PID and PD controllers

was proposed. It is worth mentioning that there is little information about studies of this type of quadcopter, and this paper could become a reference for new studies on this topic.

The application of the control theory of robot manipulators to a V–tail quadcopter, shown in this paper, is validated by simulation, obtaining as a result of a new methodology to design PD and PID controllers for stabilization of UAVs. Moreover, the stability analysis using a Lyapunov function was developed in a different way (based on the same robot manipulator theory), introducing a new variable and a new parameter that had never been used before in quadcopter stability analysis.

From the results, it can be concluded that the PID controller can keep the quadcopter operating close to the stationary state and also eliminates the error in the stable state; furthermore, the properties of the closed–loop system can be modified depending on the necessities of the application by varying the gains of the controller. The PD controller presents an error in the stable state that will not disappear as time goes on, so this can be a problem if an application with precisión is required. The SMC has a facile and rapid response, which it makes the quadcopter converge to the desired point in the space. Then, the fact that ϕ and θ angles are big can bring problems in the real world (due to the simplifications made on the model), so it needs to be validated first through experiments.

Existing knowledge of typical × structure quadcopters was applied to this specified case, proving the similarity between them and V–tail quadcopters.

It is left for future work to analyze the behavior of the V–tail quadcopter when the β angle is not 0, so it is the comparison of the performance of several configurations of β. The construction of the V–tail and the experimental validation of the theory presented in this paper is also left for upcoming projects.

REFERENCES

[1] S. N. Ghazbi, Y. Aghli, M. Alimohammadi, and A.-A. Akbari, "Quadrotors unmanned aerial vehicles: A review," *Int. J. Smart Sens. Intell. Syst.*, vol. 9, no. 1, pp. 309–333, 2016.

[2] M. H. Tanveer *et al.*, "NMPC-PID based control structure design for avoiding uncertainties in attitude and altitude tracking control of quad-rotor (UAV)," in *Proc. IEEE 10th Int. Colloq. Signal Process. Appl. (CSPA)*, Kuala Lumpur, Malaysia, Mar. 2014, pp. 117–122.

[3] J. Li and Y. Li, "Dynamic analysis and PID control for a quadrotor," in *Proc. Int. Conf. Mechatronics Autom. (ICMA)*, Beijing, China, Aug. 2011, pp. 573–578.

[4] A. H. Ahmed, A. N. Ouda, A. M. Kamel, and Y. Z. Elhalwagy, "Attitude stabilization and altitude control of quadrotor," in *Proc. 12th Int. Comput. Eng. Conf. (ICENCO)*, Cairo, Egypt, Dec. 2016, pp. 123–130.

[5] S. M. Vaitheeswaran and R. Mekala, "Non-linear attitude control methods for quadrotor MAVs—A study," in *Proc. Int. Conf. Cognit. Comput. Inf. Process. (CCIP)*, Noida, India, Mar. 2015, pp. 1–6.

[6] Lynxmotion. (2017). *Lynxmotion–VTail 400*. [Online]. Available: http://www.lynxmotion.com/c-166-vtail-400.aspx

[7] S. Khatoon, M. Shahid, I. Nasiruddin, and H. Chaudhary, "Dynamic modeling and stabilization of quadrotor using PID controller," in *Proc. Int. Conf. Adv. Comput., Commun. Inform. (ICACCI)*, New Delhi, India, Sep. 2014, pp. 746–750 [Online]. Available: https://ieeexplore.ieee.org/abstract/document/6968383/ and [Online]. Available: https://www.jmi.ac.in/upload/employeeresume/ibraheem.pdf

[8] S. F. Ahmed, K. Kushsairy, M. I. A. Bakar, D. Hazry, and M. K. Joyo, "Attitude stabilization of quad-rotor (UAV) system using fuzzy PID controller (an experimental test)," in *Proc. 2nd Int. Conf. Comput. Technol. Inf. Manage. (ICCTIM)*, Johor, Malaysia, Apr. 2015, pp. 99–104.

[9] S. H. Jeong and S. Jung, "Bilateral teleoperation control of a quadrotor system with a haptic device: Experimental studies," in *Proc. IEEE Int. Conf. Robot. Autom. (ICRA)*, Hong Kong, May/Jun. 2014, pp. 543–548.

[10] M. Hehn and R. D'Andrea, "A flying inverted pendulum," in *Proc. IEEE Int. Conf. Robot. Autom. (ICRA)*, Shanghai, China, May 2011, pp. 763–770.

[11] M. T. Hussein and M. N. Nemah, "Modeling and control of quadrotor systems," in *Proc. 3rd RSI Int. Conf. Robot. Mechatronics (ICROM)*, Tehran, Iran, Oct. 2015, pp. 725–730.

[12] G. Jithu and P. R. Jayasree, "Quadrotor modelling and control," in *Proc. Int. Conf. Elect., Electron., Optim. Techn. (ICEEOT)*, Chennai, India, Mar. 2016, pp. 1167–1172.

[13] J. Yang, Z. Cai, Q. Lin, and Y. Wang, "Self-tuning PID control design for quadrotor UAV based on adaptive pole placement control," in *Proc. Chin. Automat. Congr. (CAC)*, Changsha, China, Nov. 2013, pp. 233–237.

[14] M. Walid, N. Slaheddine, A. Mohamed, and B. Lamjed, "Modeling and control of a quadrotor UAV," in *Proc. 15th Int. Conf. Sci. Techn. Autom. Control Comput. Eng. (STA)*, Hammamet, Tunisia, Dec. 2014, pp. 343–348.

[15] H. C. T. E. Fernando, A. T. A. De Silva, M. D. C. De Zoysa, K. A. D. C. Dilshan, and S. R. Munasinghe, "Modelling, simulation and implementation of a quadrotor UAV," in *Proc. IEEE 8th Int. Conf. Ind. Inf. Syst. (ICIIS)*, Peradeniya, Sri Lanka, Dec. 2013, pp. 207–212.

[16] S. Lee, D. K. Giri, and H. Son, "Modeling and control of quadrotor UAV subject to variations in center of gravity and mass," in *Proc. 14th Int. Conf. Ubiquitous Robots Ambient Intell. (URAI)*, Jeju, South Korea, Jun./Jul. 2017, pp. 85–90.

[17] M. Herrera, W. Chamorro, A. P. Gómez, and O. Camacho, "Sliding mode control: An approach to control a quadrotor," in *Proc. Asia–Pacific Conf. Comput. Aided Syst. Eng. (APCASE)*, Quito, Ecuador, Jul. 2015, pp. 314–319.

[18] R. Kelly, V. D. Santibáñez, and A. J. P. Loría, *Control of Robot Manipulators in Joint Space*. Leipzig, Germany: Springer, 2005.

[19] J. G. Leishman, *Principles of Helicopter Aerodynamics*. New York, NY, USA: Cambridge Univ. Press, 2006.

[20] S. Lupashin, A. Schöllig, M. Sherback, and R. D'Andrea, "A simple learning strategy for high-speed quadrocopter multi-flips," in *Proc. IEEE Int. Conf. Robot. Autom. (ICRA)*, Anchorage, AK, USA, May 2010, pp. 1642–1648.

[21] Q. Ali and S. Montenegro, "Explicit model following distributed control scheme for formation flying of mini UAVs," *IEEE Access*, vol. 4, pp. 397–406, 2016.

JOSÉ J. CASTILLO-ZAMORA received the master's degree in mechanical engineering from the Tecnológico Nacional de México en Celaya in 2016. In 2015, he joined the Department of Mechanical Engineering and the Department of Mechatronics, Tecnológico Nacional de México en Celaya, as a Signature Professor. Since 2017, he has been with the Department of Mechatronics Engineering, Tecnológico Nacional de México en Celaya, where he is currently an Associate Professor. His current research field is the modeling, control and design of intelligent aerial systems, machine learning, and robot–nature interaction applications.

KARLA A. CAMARILLO-GÓMEZ received the Ph.D. degree from the Tecnologico Nacional de Mexico en la Laguna. In 2009, she joined the Tecnologico Nacional de Mexico en Celaya as a Professor, where she is currently a Professor and the Head of the research projects with the Department of Mechanical Engineering. Her current research field is focuses on modeling and control of robots, control of nonlinear systems, stability analysis of nonlinear systems, development of rehabilitation systems, humanoid robots, and assembly automatization and applications of vision control on industrial processes. She is a member of the Mexican Association on Robotics and Industry (AMRob) and the Co-Chair of HuroCup of Federation International of Robo-Sports Association (FIRA). She received several fellowships and awards on robotics by AMRob and FIRA.

GERARDO I. PÉREZ-SOTO received the Ph.D. degree from the Unviersidad de Guanajuato. In 2013, he joined the Universidad Autonoma de Queretato (UAQ) as an Assistant Professor. He is currently a Professor of the Facultad de Ingenieria, UAQ. His current research field focuses on theoretical kinematics, humanoid robots, mobile robots, and assembly automatization and applications of mechanical engineering on industrial processes. He is a member of the Mexican Association on Robotics and Industry. He received several fellowships and awards including the A. T. Yang Memorial Award in Theoretical Kinematics as the Best Paper by the American Society of Mechanical Engineering in 2007 and 2011. He is with the National System of Researchers, CONACyT, Mexico.

JUVENAL RODRÍGUEZ-RESÉNDIZ (SM'13) received the Ph.D. degree from Querétaro State University, México, in 2010. In 2012, he joined West Virginia University as a Visiting Professor. Since 2008, he has been a Professor with Querétaro State University. He received several awards for his contributions in developing education technology. He focused on industrial and academic automation projects for 15 years. He is currently the Chair of the Engineering Automation Program, the Master in Automation Program, and the Director of Technologic Link with Querétaro State University. He is with the Mexican Academy of Sciences, the National Research Academy in México, and seven associations regarding engineering issues. He was the President of the IEEE Querétaro Section.

• • •